

## Supporting Information

# A New Approach to Understand Cassie State of Liquids on Superamphiphobic Materials

Tao Wang, Jing Cui, Shenshen Ouyang, Weihao Cui and Sheng Wang\*

*\*e-mail: wangsheng571@hotmail.com*

*Key Laboratory of Advanced Textile Materials and Manufacturing Technology, Ministry of  
Education, Zhejiang Sci-Tech University, Hangzhou 310018, P. R. China.*

*E-mail: wangsheng571@hotmail.com*

## Table of Contents

- S1. Surface wettability of Te@C-SiO<sub>2</sub> nanocomposites
- S2. TGA
- S3. EDS
- S4. XPS
- S5. Theoretical discussion about the superamphiphobic surface
- S6. N<sub>2</sub> adsorption-desorption isotherm and pore size distributions of Te@C
- S7. N<sub>2</sub> adsorption-desorption isotherm and pore size distributions of P30
- S8. Physical structural data of the samples.
- Movie Legends

## S1. Surface wettability of Te@C-SiO<sub>2</sub> nanocomposites

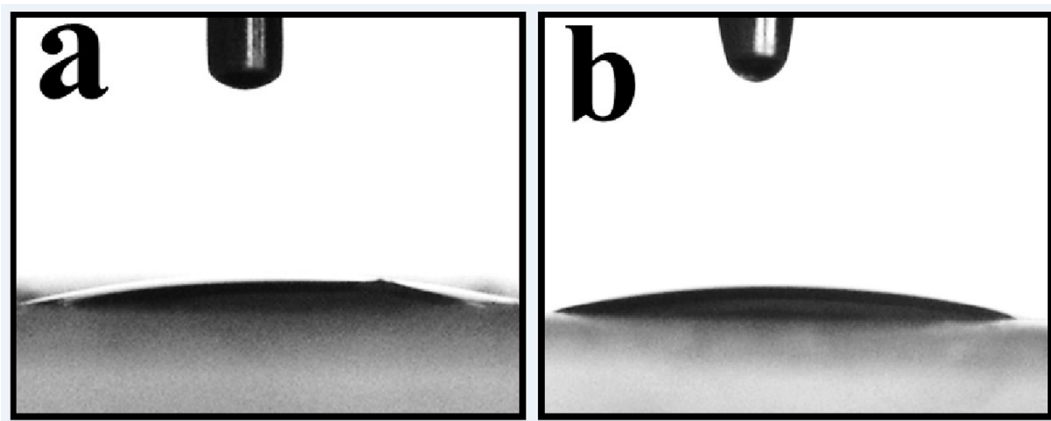
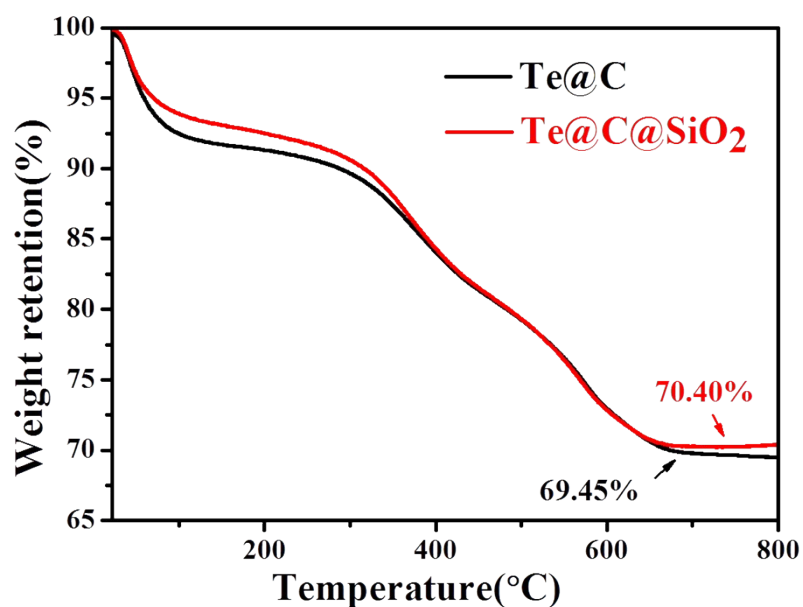


Figure S1: Photographs of water (a) and *n*-hexadecane (b) droplets sitting on the Te@C-SiO<sub>2</sub> coated glass plate, respectively.

## S2. Thermogravimetric analysis (TGA) analysis of Te@C-SiO<sub>2</sub>

Thermogravimetric analysis (TGA) analysis was employed to quantify the amount of SiO<sub>2</sub> NPs that had been grown on the surfaces of the Te@C nanofibers. Te@C was used as the reference sample. Both samples show similar profiles. The weight loss below 100 °C is attributed to evaporation of adsorbed water on the samples. The greater weight loss can be attributed to the decomposition of hydrothermal carbon layer on Te nanowires obtained by oxidation between 100 °C and 650 °C. Deducted the amount of Te, the weight content of the SiO<sub>2</sub> NPs can be calculated as ~8.1% for Te@C-SiO<sub>2</sub>.



**Figure S2:** TGA curves of Te@C (black line) and Te@C-SiO<sub>2</sub> (red line).

### S3. EDS

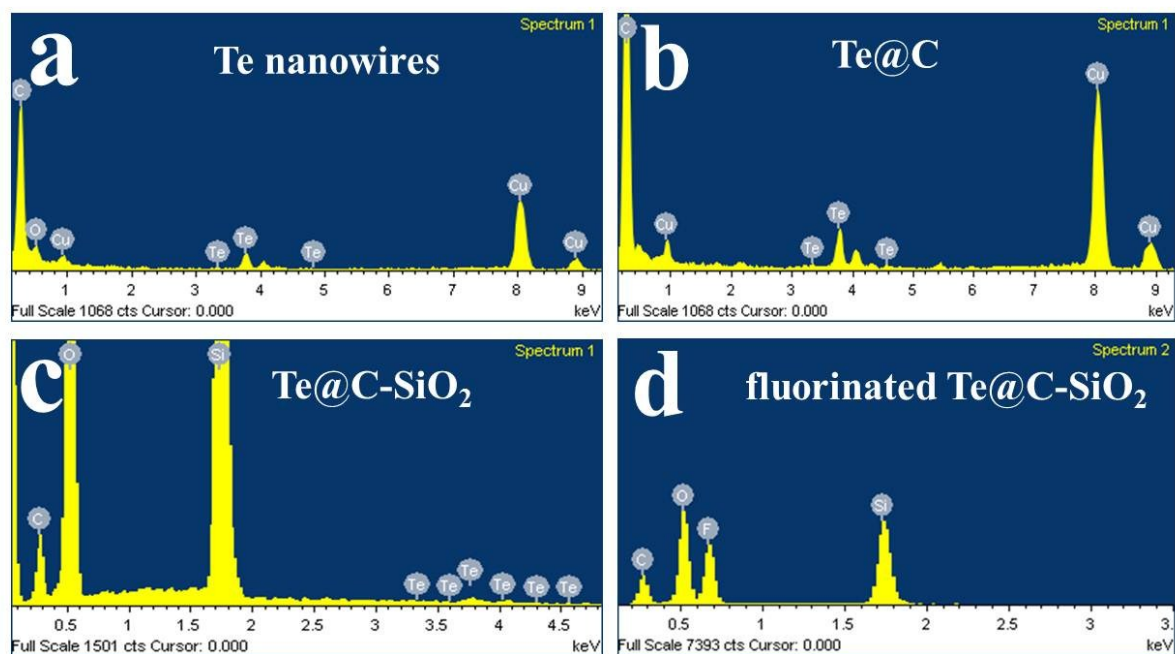


**Figure S3.** EDS of the obtained products at different reaction processes.

## S4. XPS

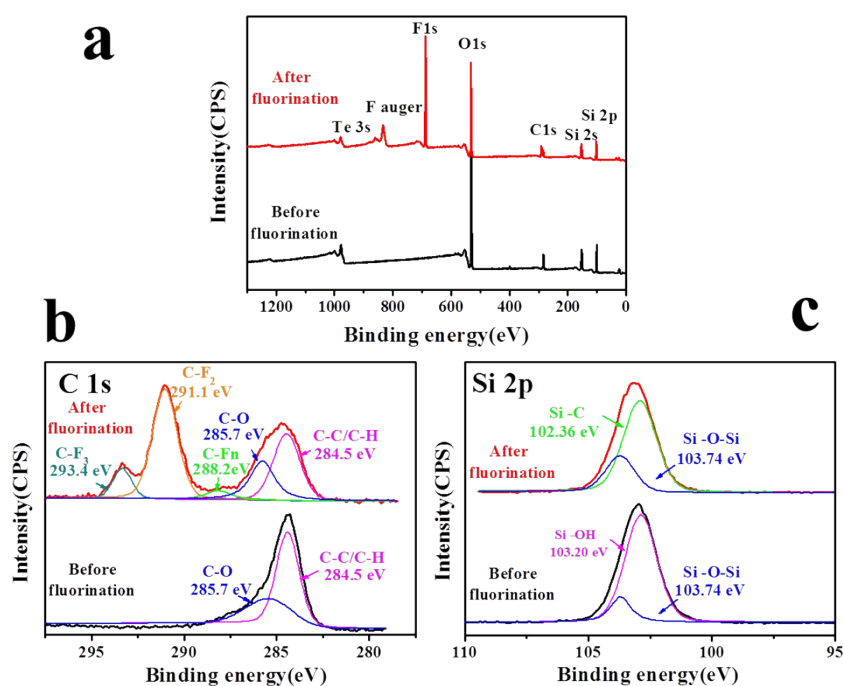


**Figure S4.** XPS spectra of the Te@C-SiO<sub>2</sub> nanocomposite surfaces before and after fluorination. (a) XPS survey spectra, XPS core level spectra of (b) the C 1s peaks and (c) Si 2P peaks.

Figure S4 shows the survey spectra of the Te@C-SiO<sub>2</sub> nanocomposites surface before and after fluorination, which clearly revealed the presence of elements such as C, O, F, and Si. It can be seen that after fluorination, signal corresponding to fluorine (F 1s, 688.26 eV) was appeared in the spectrum.

Figure 4S (b) and (c) showed the XPS results of the high resolution C 1s and Si 2p spectrum with and without PFOTS treatment. Deconvolution of the C 1s signal into its several components confirms the graft of a semi-fluoroalkyl groups on the nanocomposites. Before fluorination the main peak was centered between 285.7 and 284.5 eV, which was originated from the hydrothermal carbon layer. A completely different XPS C 1s spectrum was observed after fluorination, where the main peak is centered between 291 and 293 eV. The deconvolution of the C 1s spectrum allowed the assignment of the signals centered at 293.4, 291.1, and 288.2 eV to CF<sub>3</sub>, CF<sub>2</sub>, CF<sub>n</sub>, respectively.<sup>1,2</sup> Before fluorination the loaded silica particles mainly exhibited Si 2p signals at a binding energy of 103.2 eV for Si-O-Si bond and 103.7 eV for Si-OH group. After fluorination, Si-OH group disappeared while a peak of Si-C bond appeared at 102.36 eV, indicating the fluoroalkyl grafted SiO<sub>2</sub> NPs have been successfully obtained.<sup>3</sup>

## S5. Theoretical discussion about the superamphiphobic surface

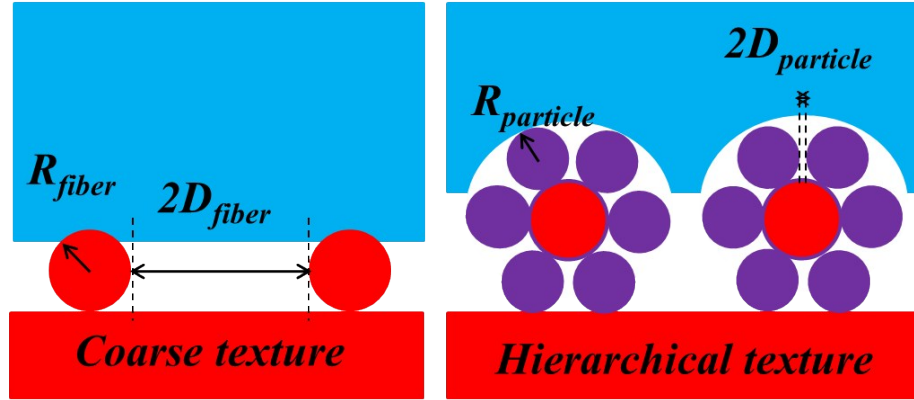


**Figure S5.** Schematics of a liquid droplet in the Cassie-Baxter state on a coarse textured surface and a hierarchically textured surface, respectively.

Tuteja et al. introduced a dimensionless parameter, the spacing ratio  $D^*$ , to predict the value of apparent contact angle CA ( $\theta^*$ ) of superamphiphobic surfaces. For substrates possessing a predominantly cylindrical fibers texture,  $D_{fiber}^* = (R + D)/R$ , while for substrates possessing a predominantly spherical texture,  $D_{particle}^* = [(R + D)/R]^2$ . Here, R is the radius of the cylindrical fibers (or sphere) and 2D is the inter-fiber (or inter-sphere) spacing (see Figure S5).

Therefore, the Cassie-Baxter relation (when a liquid droplet is in the Cassie-Baxter state, the apparent contact angles can be determined using the Cassie-Baxter relation shown in Equation (1)<sup>4,5</sup>) may be rewritten for surfaces possessing a fiber (Equation (2)) or a spherical (Equation (3)) texture as:<sup>4,5</sup>

$$\cos\theta^* = f_{SL}\cos\theta + f_{LV}\cos\pi = f_{SL}\cos\theta - f_{LV} \quad (1)$$

$$\cos\theta_{fiber}^* = -1 + \frac{1}{D_{fiber}^*}[\sin\theta + (\pi - \theta)\cos\theta] \quad (2)$$

$$\cos\theta_{particle}^* = -1 + \frac{1}{D_{particle}^*}\left[\frac{\pi}{2\sqrt{3}}(1 + \cos\theta)\right] \quad (3)$$

Considering a hierarchically structured surface composed of spherical particles on top of the underlying cylindrical fiber texture. The Cassie-Baxter relationship can be rewritten recursively as:

$$\cos\theta_{hierarchical}^* = -1 + \frac{1}{D_{fiber}^*} \times [\sin\theta_{particle}^* + (\pi - \theta_{sphere}^*)\cos\theta_{particle}^*] \quad (4)$$

In our study, surface roughness is related to the dual scale structure of Te@C-SiO<sub>2</sub>, which is the combination of the coarser texture derived from Te@C fibers and the finer texture from spherical SiO<sub>2</sub> NPs.

For another dimensionless parameter, robustness factor  $A^*$ , which is the ratio of the breakthrough pressure ( $P_{breakthrough}$ ) required to force the transition from the Cassie state to the Wenzel state and the reference pressure ( $P_{ref}$ ) across the interface from the effects of gravity and the Laplace pressure within the droplet. The robustness factors for cylindrical surface (Equation (5)), a spherical surface (Equation (6)) and a hierarchically structured surface composed of spherical particles on top of the underlying cylindrical fiber texture texture (Equation (7)) are given as:<sup>6</sup>

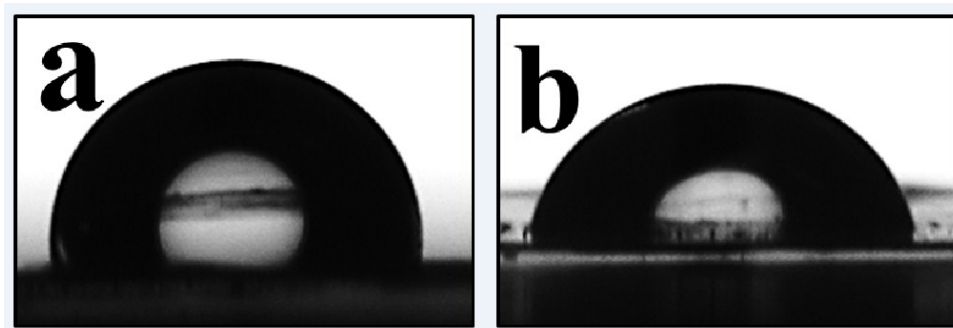
$$A_{fiber}^* = \frac{P_{breakthrough}}{P_{ref}} = \frac{l_{cap} (1 - \cos \theta)}{R(D_{fiber}^*)(D_{fiber}^* - 1 + 2\sin \theta)} \quad (5)$$

$$A_{particle}^* = \frac{P_{breakthrough}}{P_{ref}} = \frac{2\pi l_{cap} (1 - \cos \theta)}{R(2\sqrt{3}D_{particle}^*)(\sqrt{D_{particle}^*} - 1 + 2\sin \theta)} \quad (6)$$

$$A_{hierarchical}^* = \frac{l_{cap} (1 - \cos \theta_{particle}^*)}{R(D_{fiber}^*)(D_{fiber}^* - 1 + 2\sin \theta_{particle}^*)} \quad (7)$$

According to Tuteja, substrates on which the robustness factor  $A^* \leq 1$  for a given contacting liquid cannot support a composite interface. On the other hand, values of  $A^*$  significantly greater than unity imply the formation of a robust composite interface that can withstand high breakthrough pressures. In our system, for all the sample:  $A^* > 1 \times 10^4$  (for water) and  $A^* > 1 \times 10^3$  (for *n*-hexadecane).

Following photographs are the contact angle of the liquid drops (water and *n*-hexadecane) deposited on a fluorinated smooth silicon wafer, respectively.



CA<sub>water</sub> = 100°

CA<sub>hexadecane</sub> = 75°

## S6. N<sub>2</sub> adsorption-desorption isotherm and pore size distributions of Te@C

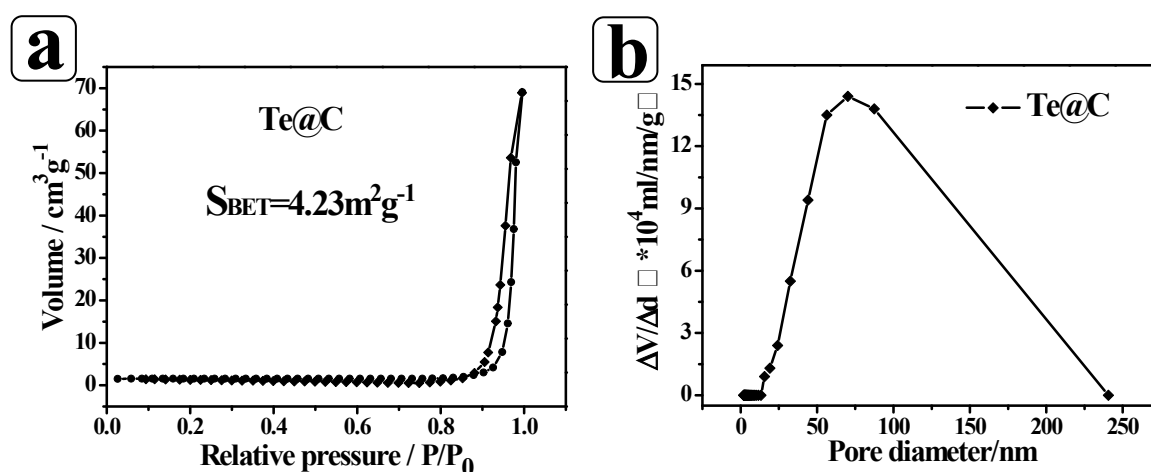


**Figure S6.** (a) Nitrogen adsorption-desorption isotherms of Te@C; (b) The corresponding pore size distribution of the sample.

There is a little difference between Te@C and Te@C coated with a layer of SiO<sub>2</sub> (sample F30-P0,  $D_{sphere}^* = 0$ , coarser texture) either in  $S_{BET}$  or in pore size distribution (a slight decrease of Te@C@SiO<sub>2</sub> is owing to that coating of SiO<sub>2</sub> layer caused a slight shrinkage of Te@C fiber), which indicates that coating of SiO<sub>2</sub> layer has almost no influence on Te@C fibers. Both the nanofibers exhibited a wide pore size distribution ranging from approximately 20 to 200 nm, which was attributed to the porosity derived from coarser texture.

S7. N<sub>2</sub> adsorption-desorption isotherm and pore size distributions of P30.

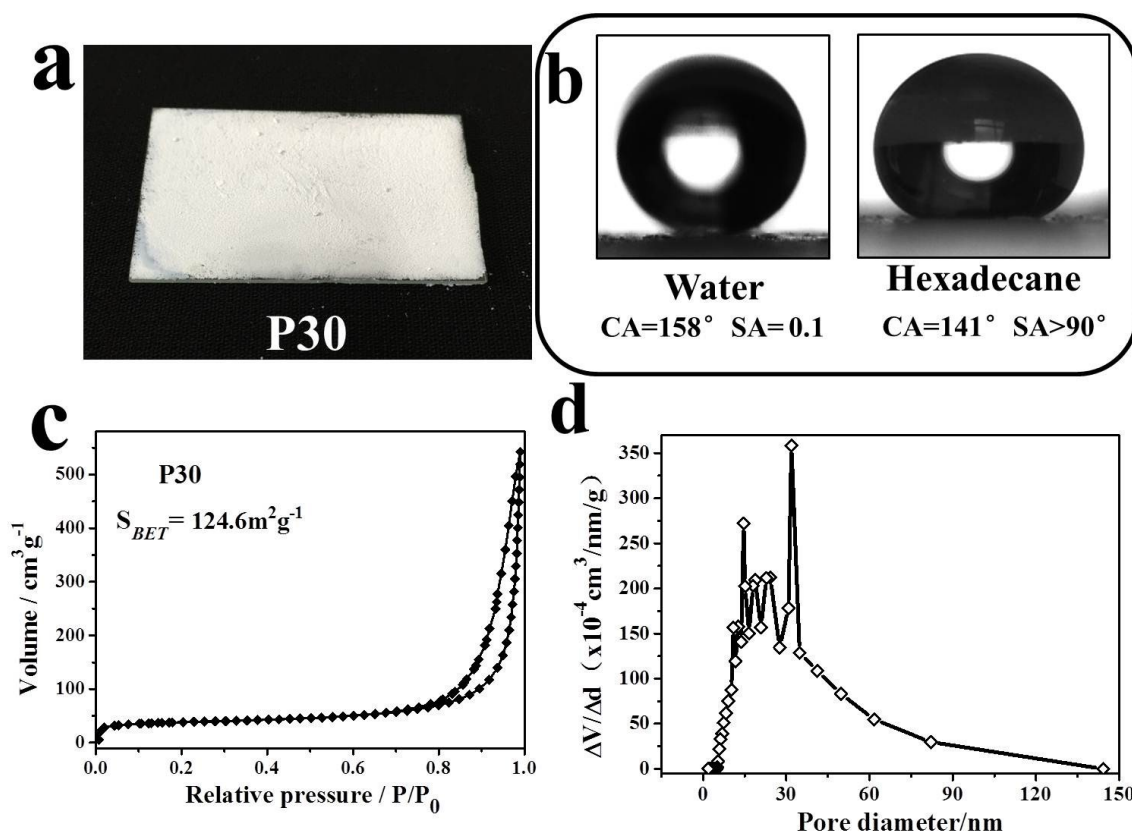


**Figure S6.** (a) Digital photographs of the P30 coatings on glass slide; (b) Profile photographs of water, *n*-hexadecane; (c) Nitrogen adsorption-desorption isotherms of P-30; (d) The corresponding pore size distribution of the sample.

## S8. Physical structural data of the samples.

**Table S3. Physical structural data of the samples.**

Sample	$S_{BET}$ (m <sup>2</sup> /g)	$V_{total}$ (mL/g)	$V_{meso}$ (mL/g)	$V_{macro}$ (mL/g)
F30-P0	5.05	0.12	0.02	0.10
F30-P50	33.15	0.17	0.07	0.10
F30-P40	40.16	0.24	0.09	0.15
F30-P30	63.17	0.39	0.12	0.26
F80-P30	13.17	0.05	0.02	0.03
F130-P30	16.19	0.13	0.07	0.06
F30-P10	77.32	0.53	0.23	0.30
F30-P20	56.16	0.17	0.10	0.07

$S_{BET}$ , BET surface area;  $V_{total}$ ,  $V_{micro}$  and  $V_{meso}$  primary total pore and microporous volume and mesoporous volume evaluated by the DFT method, respectively.

## REFERENCES

1. Yokoi, N.; Manabe, K.; Tenjimbayashi, M.; Shiratori, S. *ACS Appl. Mater. Interfaces* **2015**, *7*, 4809-4816.
2. Rangel, T. C.; Michels, A. F.; Horowitz, F.; Weibel, D. E. *Langmuir* **2015**, *31*, 3465-3472.
3. He, Z.; Ma, M.; Lan, X.; Chen, F.; Wang, K.; Deng, H.; Zhang, Q.; Fu, Q. *Soft Matter*, **2011**, *7*, 6435-6443.
4. Choi, W.; Tuteja, A.; Chhatre, S.; Mabry, J. M.; Cohen, R. E.; McKinley, G. H. *Adv. Mater.* **2009**, *21*, 2190-2195.
5. Chhatre, S. S.; Choi, W.; Tuteja, A.; Park, K. C.; Mabry, J. M.; McKinley, G. H.; Cohen, R. E. *Langmuir* **2010**, *26*, 4027-4035.
6. Tuteja, A.; Choi, W.; Mabry, J. M.; McKinley, G. H.; Cohen, R. E. *Proc. Natl Acad. Sci. USA* **2008**, *105*, 18200-18205.

## Movie Legends

Movie S1. This video illustrates the roll-off of water (blue) and *n*-hexadecane (pink) droplets on hierarchically structured superamphiphobic surface (F30-P30 spray coated glass slide).

Movie S2. This video illustrates the roll-off of water (blue) and *n*-hexadecane (red) droplets on hierarchically structured superamphiphobic bulk material (F30-P30 shaped bulk).

Movie S3. This video illustrates the bouncing of a 3  $\mu\text{L}$ /2  $\mu\text{L}$  (water/*n*-hexadecane) droplets that is dropped on the hierarchically structured superamphiphobic surface (F30-P30 spray coated glass slide).